

- (accepted to J. Electrochem. Society  
need modifications and an up-to-dating background)

**A MODEL FOR THE INITIATION OF CREVICE CORROSION  
IN GRADE-12 TITANIUM IN A BRINE SOLUTION\***

**T. M. Ahn**

**Department of Nuclear Energy  
Brookhaven National Laboratory  
Upton, New York, 11973**

**Key Description: Titanium, Crevice Corrosion Model, Diffusion, Migration**

*Main/ Legacy - 70.*

## ABSTRACT

A model is developed for the initiation of crevice corrosion of Grade-12 titanium in high temperature brine. It is based on experimental results from immersion tests, surface analyses and electrochemical measurements. During crevice corrosion, the anode potential initially increases due to the growth of a corrosion barrier oxide which consumes the oxygen inside the crevice, until the maximum potential is reached. At the maximum potential the barrier oxide stops growing, and the following potential drops are governed by the solution chemistry change within the crevice. The potential changes associated with the solution chemistry include (1) a potential drop caused by an oxygen concentration change (2) an ohmic potential drop (3) a potential rise due to pH changes and (4) a potential rise due to excess proton generation. For the growth of oxide, a simple mass balance gives the potential rise as the oxide thickness is increased. Simplified diffusion equations for the concentrations of oxygen, proton and anions are used to estimate the chemistry change inside the crevice. Diffusion caused by the concentration gradient and potential field within the crevice are considered. For the chemistry change, the potential is calculated using the Nernst equation. Potential changes are compared to experimental values. The comparison allows an estimate to be made of the concentration gradient distance. The final equations attained are used to draw domains for crevice corrosion initiation on a temperature/anion concentration diagram. The calculated domains are consistent with measured domains available in the literature. Also the equations developed provide a technique for estimating the solution chemistry inside the crevice as a function of time and the final crevice chemistry at equilibrium. Since the calculated (limiting) crevice chemistry is very aggressive, crevice corrosion is inevitable over a wide range of conditions.

## FIGURES

1. Experimental potential (open circles) and "fitted" potential (solid line) of coupled Grade-12 titanium crevices in aerated neutral brine at 150°C.
2. The calculated concentration profiles in the crevice at various testing times for a current density of 10  $\mu\text{A}/\text{cm}^2$ .
3. Immunity domains for crevice corrosion at various service times for Grade-12 titanium in a simulated rock salt brine. The critical anion concentration assumed for passivity breakdown is 190,000 ppm.
4. Immunity domains in temperature and pH necessary for passivity breakdown for CP titanium.<sup>18</sup>

## TABLES

1. Calculated limiting chloride concentrations at infinite time in the crevice of Grade-12 titanium in aerated neutral Brine A at 150°C.

## 1. INTRODUCTION

As shown in the previous two papers,<sup>1,2</sup> immersion tests, surface analyses and electrochemical studies have shown that macroscopic concentration cell formation is responsible for Grade-12 titanium crevice corrosion in a simulated rock salt brine at 150°C. Cell formation is accompanied by oxygen depletion, a potential drop, anion accumulation and acidification inside the crevice. This leads to pit initiation. To quantify the crevice corrosion process, surface films have been analyzed and the anode and cathode reactions have been studied using a specially-designed cell in which the two electrodes are physically separated. The anode potential, current flow from cathode to anode and pH inside the crevice have been monitored. In this paper, we present a simplified model to explain the results of the surface analyses and the electrochemical measurements.

Among the five models available to explain crevice corrosion in the literature,<sup>3-7</sup> two comprehensive models have been chosen for study: (1) an electrochemical/hydrodynamic model<sup>6</sup> considering sample geometry effects and (2) an electrochemical model with a minor modification for hydrodynamic effects.<sup>4</sup> Our experimental design may be interpreted better by the latter model<sup>4</sup> for the following reasons: (1) the sample size is large enough and the dissolution rates are fast enough to minimize diffusion effects i.e., sample geometry effects, (2) the crevices used in the present work are obtained by tightly joining two coupons. Since the crevice gap will not be constant on a local scale because of surface imperfections, the model with sample geometry effects<sup>6</sup> is less applicable. Also, the former model has only a numerical solution, so it is difficult to visualize the functional dependence of mass

balance and to extrapolate behavior to extended times. On the other hand, the latter model does not consider hydrodynamic mass balance quantitatively and excludes surface characterization results. To resolve these shortcomings, we present a simplified model based on our experimental observations.

## 2. UNDERLYING MECHANISMS AND BASIC ASSUMPTIONS

The anode potential increases continuously during the growth of a barrier oxide (anatase form of  $TiO_2$ ) until the maximum potential is reached. The relation of the oxide thickness and the electrode potential is linear.<sup>8,9</sup> After the maximum potential is reached, the barrier oxide stops growing and the following potential drops are governed mainly by solution chemistry changes in the crevice. The solution chemistry changes from the initial state beginning by the consumption of oxygen inside the crevice and by the subsequent anode-cathode separation stage which causes accumulation of protons and anions inside the crevice. The potential change caused by the solution chemistry modification is obtained by considering (1) a potential drop caused by an oxygen concentration change,<sup>10,11</sup> (2) an ohmic potential drop,<sup>5,12</sup> (3) a potential rise due to pH changes,<sup>11</sup> and (4) a potential rise due to excess proton generation.<sup>13</sup> Because of the solution chemistry change, a pitting environment forms. Contribution (2) is approximately negated by contribution (3) based on calculations for estimating the ohmic potential.<sup>11</sup> Also, contribution (4) is, typically, negligible because of the conservation of charge neutrality.<sup>13</sup> Therefore, after the maximum potential is reached, the effects of oxygen depletion are dominant and complete oxygen depletion is an important prerequisite for pit initiation since a pit initiates when the potential becomes low while the oxide thickness remains constant.<sup>14</sup> We assume

that this oxygen depletion stage is the critical condition for the initiation of crevice corrosion. In the preceding paper, the initiation times for varying proton and anion concentrations are shown to be similar, supporting our assumption that oxygen depletion is the critical condition for the initiation of crevice corrosion. We exclude the consideration of the complicated kinetic process of monolayer formation at the Flade potential in pits. This is a conservative criterion for the initiation condition.

During mass transport, protons are generated in the crevice by the anode-cathode separation process. Diffusion and field-enhanced diffusion (migration) terms decrease the proton concentration. Oxygen is consumed but is still supplied by diffusion from outside the crevice. Anions migrate into the crevice to neutralize the protons generated, while the accumulated anions are moved out by diffusion.

Instead of adopting partial differential equations and boundary conditions for mass balance calculations, we use the effective concentration gradient distance,  $\delta$ , which allows us to describe the diffusion equation in simple terms. We use a linear concentration or potential gradient across this value  $\delta$ . This is a valid assumption when  $\delta$  is very small compared to the sample size. In the calculation of potential using the Nernst equation, the concentration term is used instead of the activity. For migration calculations, the potential term is obtained from the anion concentration on the basis of assumptions used by Vermilyea.<sup>12</sup> Our major consideration concerns the proton and chloride ions since they are the major ions present. Other types of anion are in small concentrations and their diffusivities are slower or, at most,

close to that for chloride ions.<sup>15</sup> Therefore, chloride and proton concentrations are considered to determine the passivity breakdown condition.

### 3. FORMULATION OF EQUATIONS AND COMPARISON TO EXPERIMENTAL RESULTS

The anode potential rise during the growth of barrier oxide is given by the following mass balance relationship:

$$V(\text{oxide}) = V_1 + I_p t M / (c \rho F) \quad (1)$$

where  $\rho$  is the density of the anatase form of  $\text{TiO}_2$ ,  $c$  is a proportionality constant (8,9),  $I_p$  is the passive current estimated from the maximum potential observed,  $t$  is the time,  $M$  is the molecular weight of  $\text{TiO}_2$ ,  $F$  is the Faraday constant and  $V_1$  is the initial potential. We have used the initial value of potential as that measured at the time when appreciable current flow ( $\sim 1 \mu\text{A}$  range) is observed. The potential drop due to the oxygen concentration change may be approximated by the Nernst equation:<sup>10,11</sup>

$$V(\text{O}_2) = V_1 + \frac{RT}{F} \ln \left( \frac{C(\text{O}_2)}{C_1(\text{O}_2)} \right) \quad (2)$$

where  $C_1(\text{O}_2)$  is the initial oxygen concentration and  $C(\text{O}_2)$  is the oxygen concentration at time  $t$ .  $C(\text{O}_2)$  is obtained by a simplified diffusion equation:

$$C(\text{O}_2) = C_1(\text{O}_2) - \frac{2 I_p t}{H F} + \frac{2 D_{\text{O}_2} t}{x \delta} [C_1(\text{O}_2) - C(\text{O}_2)] \quad (3)$$

where  $x$  is the crevice depth,  $H$  is the crevice gap size,  $\delta$  is the effective length of the oxygen concentration gradient within the crevice, and  $D_{\text{O}_2}$  is

the oxygen diffusivity. The second term represents oxygen concentration consumed and the third term represents oxygen concentration by diffusion inflow. Upon separation of the anodic and cathodic areas, a current,  $I$ , flows from the cathode to the anode resulting in the accumulation of protons, and in the migration of chloride ions to the crevice. The accumulated concentrations of protons  $C(H^+)$  and chloride ions  $C(Cl^-)$  are given by the following mass balance equations:

$$C(H^+) = C_1(H^+) + \frac{2 I t}{F H} - \frac{2 D_{H^+} t}{x \delta} [C(H^+) - C_1(H^+)]$$

$$- \frac{2 D_{H^+} t C(H^+)}{x \delta} \ln \left( \frac{C(H^+)}{C_1(H^+)} \right) \quad (4)$$

$$C(Cl^-) = C_1(Cl^-) - \frac{2 D_{Cl^-} t}{x \delta} [C(Cl^-) - C_1(Cl^-)]$$

$$+ \frac{2 D_{Cl^-} t C_1(Cl^-)}{x \delta} \ln \left[ \frac{C(H^+)}{C_1(H^+)} \right] \quad (5)$$

where  $C_1(H^+)$  and  $C_1(Cl^-)$  are initial concentrations of proton and chloride ion, respectively, and  $D_{H^+}$  and  $D_{Cl^-}$  are diffusivities of the proton and the chloride ions, respectively. The above two equations have diffusion terms arising from the concentration gradient and from field-enhanced diffusion (migration). The field potential is approximated using the proton concentration.<sup>12</sup> From these two equations, the ohmic potential drop may be given by:<sup>5,12</sup>

$$V(\text{ohmic}) = V_1 + \frac{RT}{F} \ln \left[ \frac{C_1(\text{HCl})}{C(\text{HCl})} \right] \quad (6)$$

where  $C_1(\text{HCl})$  and  $C(\text{HCl})$  are HCl concentrations at  $t=0$  and  $t$ , respectively. The potential change due to the pH decrease is approximately the negative value of Equation (6). Therefore, the net effect is from the oxygen concentration [Equation (2)].

The best fit to our experimental data (neutral Brine A) is shown in Figure 1 for  $\delta = 0.3$  cm (effective distance of concentration gradient),  $I_p = 7.6 \times 10^{-10}$  amp/cm<sup>2</sup> (passive current with oxygen reduction),  $c = 2.5 \times 10^{-7}$  cm/volt<sup>9,10</sup> (a proportionality constant between oxide thickness and electrode potential), crevice depth = 2.54 cm, crevice gap = 2  $\mu$ m, an oxygen diffusivity (cm<sup>2</sup>/sec) of  $0.0821 \exp(-2440/T)$ ,<sup>16</sup> a proton diffusivity (cm<sup>2</sup>/sec) of  $0.02838 \exp(-1700/T)$ ,<sup>16</sup> chloride diffusivity (cm<sup>2</sup>/sec) of  $0.0508 \exp(-2327/T)$ ,<sup>16</sup> and an anatase density of 3.84 gm/cc.<sup>17</sup> Very little change occurs in Figure 1 with a current variation from 0.24 to 10  $\mu$ A/cm<sup>2</sup>, because the main potential drop arises from oxygen effects. Figure 2 shows the concentration profiles in the crevice at various testing times for a current density of 10  $\mu$ A/cm<sup>2</sup>. Because the brine solution has a near saturated Cl<sup>-</sup> ion concentration, the calculated large value indicates some types of precipitates which may form. Also, the low pH level indicates that the actual pH at higher temperatures is much lower than that measured at room temperature (experimental values vary from 2.8 to 4.5). Two curves for oxygen concentrations are shown for different crevice heights. As expected, an increased crevice gap size delays the oxygen depletion time significantly. This is also true for increasing crevice area.

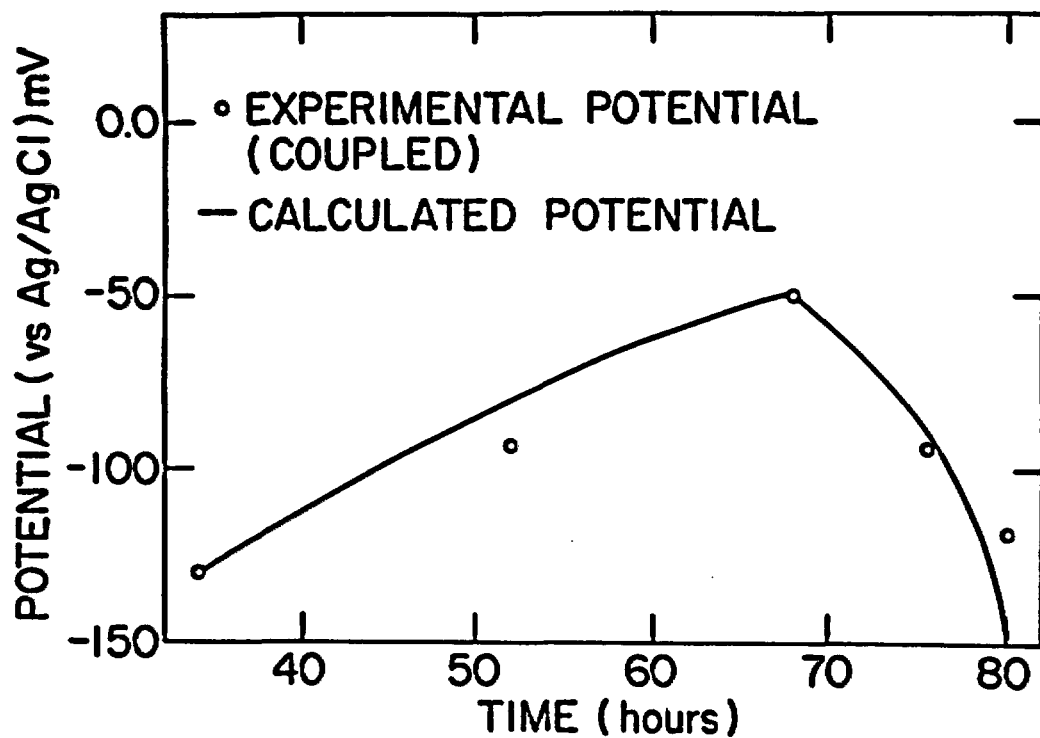


Figure 1. Experimental potential (open circles) and "fitted" potential (solid line) of coupled Grade-12 titanium crevices in aerated neutral brine at 150°C.

Data fitting was not performed for the results obtained in the solution varying concentrations. During the initiation period, the essential features for all cases were identical within the scatter of the experimental values. The detailed comparisons are out of the scope of present works.

The solution within a crevice will tend to have a limiting composition as the corrosion time approaches infinity. From the predictive equations [Equations (3), (4) and (5)] the limiting concentration is obtained by dividing each term by time  $t$  and letting time approach infinity. Calculation shows that there is no limiting pH and oxygen concentration, and these parameters can theoretically fall to extremely low values within the crevice. Table 1 shows the computed limiting values of  $\text{Cl}^-$  concentration within the crevice for assumed values of pH. Note that these  $\text{Cl}^-$  concentration levels are in excess of  $10^6$  ppm which is not physically possible. However, the analytical approach serves to show that extremely high levels of chloride will accumulate with time.

Table 1. Calculated limiting chloride concentrations at infinite time in the crevice of Grade-12 titanium in aerated neutral Brine A at 150°C.

| Limiting pH                                | -1        | 0         | 1         | 2         | 3         |
|--------------------------------------------|-----------|-----------|-----------|-----------|-----------|
| Limiting $\text{Cl}^-$ Concentration (ppm) | 3,690,560 | 3,279,590 | 2,815,420 | 2,377,850 | 1,940,280 |

The initial  $\text{Cl}^-$  concentration is 190,000 ppm. A  $\text{Cl}^-$  concentration of more than  $10^6$  ppm implies that there is no practical limitation on chloride ion accumulation as time progresses.

To study the effects of initial chloride concentration and temperature, a calculation was performed based on the above discussion. With  $\text{pH} = -1.19$  in Figure 2 and the critical value of chloride ion concentration for passivity breakdown taken to be 190,000 ppm (near saturation of brine with chloride ions), a map is drawn in the space of temperature and the initial chloride concentration  $C_i(\text{Cl}^-)$  necessary to attain the critical concentration at various times. A calculation was performed using Equation (5) by setting  $C(\text{Cl}^-) = 190,000$  ppm and  $\text{pH} = -1.19$  for  $C(\text{H}^+)$ . As expected, smaller amounts of initial chloride ions are needed at higher temperatures for the initiation of crevice corrosion. Such domains have been experimentally determined in unalloyed Ti and Ti-Pd alloys exposed to dilute sodium chloride solutions.<sup>18</sup> Therefore, our simple formulation is promising. Further, this calculation permits the extrapolation to long term behavior. Inside the unshaded area of Figure 3, crevice corrosion occurs while the hatched area shows immunity to crevice corrosion. The boundary between the two domains is affected by the corrosion time with the domain for crevice corrosion becoming larger as corrosion times are increased. At infinite corrosion time, the boundary becomes a straight line designated by  $C_{th}$ , below which crevice corrosion does not occur even at infinite time.

Note that the curves in Figure 3 have been calculated on the basis of a corrosion current which is independent of test temperature. When the temperature dependence of the current is considered, the curves in this figure depend more strongly on the chloride concentration. Also, the model developed shows that there will be a temperature limit,  $T_{th}$ , below which mass flow in the corrosion system ceases. Since the calculated  $T_{th}$  is lower than the

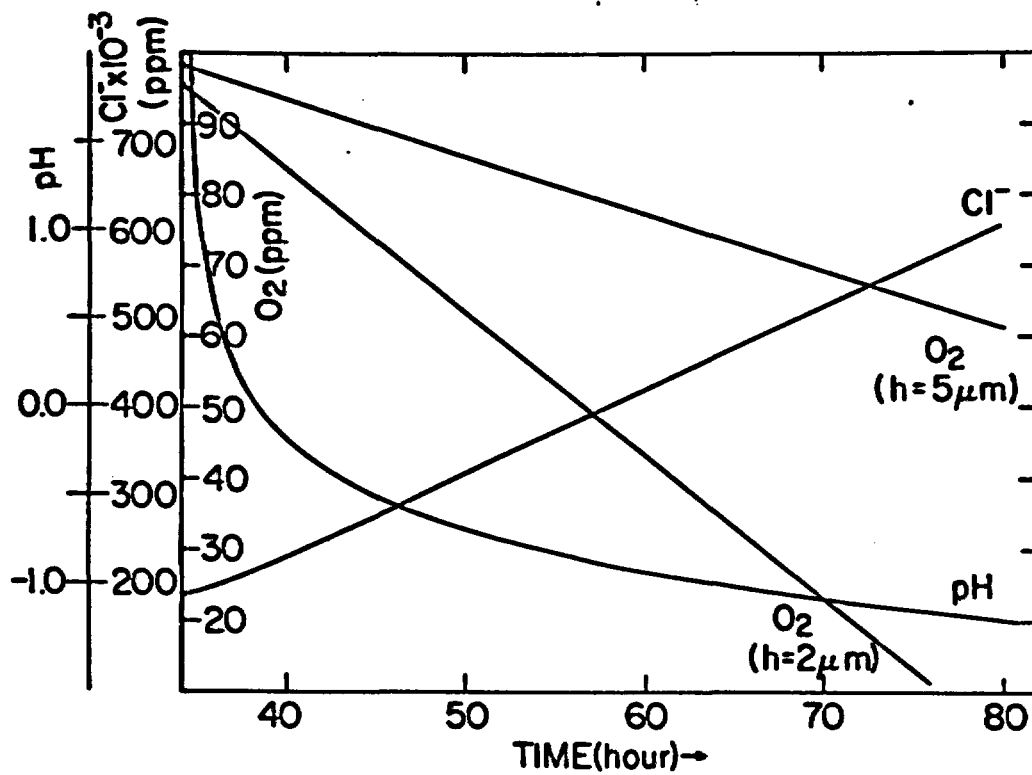


Figure 2. The calculated concentration profiles in the crevice at various testing times for a current density of  $10 \mu\text{A}/\text{cm}^2$ .

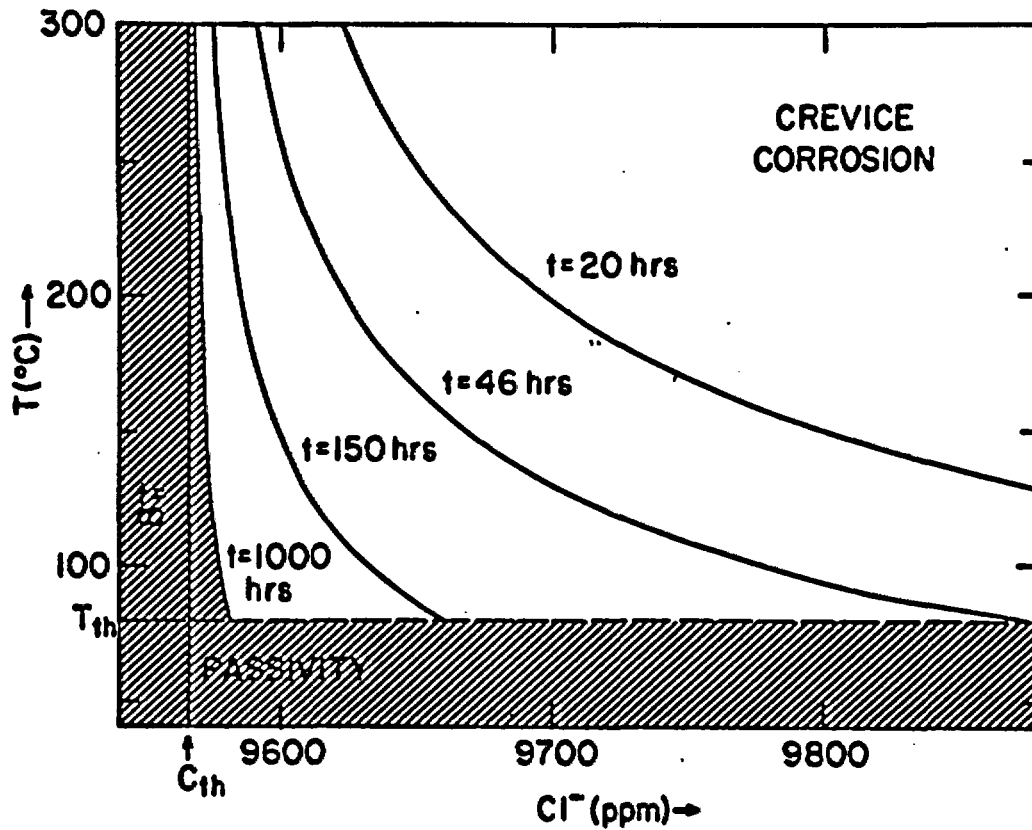


Figure 3. Immunity domains for crevice corrosion at various service times for Grade-12 titanium in a simulated rock salt brine. The critical anion concentration assumed for passivity breakdown is 190,000 ppm.

freezing point of the test solution, it does not have a significant meaning at these low temperatures.

#### 4. DISCUSSION

In the above crevice corrosion analysis, we have used a linear variation of the concentration gradient introducing an adjustable parameter  $\delta$  (effective concentration gradient distance). Severe crevice corrosion at the edges of test specimens supports the assumption that  $\delta$  is very small compared to the specimen size. This is also predicted in our calculations. We have used concentration instead of activity in the calculation of potential. The present experiments do not provide activity coefficients for various ions at high temperatures. However, since most of the activity coefficients are incorporated in logarithmic terms for the potential calculation, the adjustable parameter  $\delta$  will not significantly change with variations in the activity coefficient.

We have not calculated the pH necessary for breaking down of passivity as a function of temperature mainly because we do not have a value for  $I$  in Equation (4) as a function of temperature and pH.  $I$  values are known to be a strong function of temperature and pH. Nevertheless, we could see that the lower pH is necessary at lower temperature qualitatively when the dependence of  $I$  on temperature and pH is stronger than the dependence of diffusivity on temperature. This was observed in the experiment also (Figure 4).<sup>18</sup> When the  $I$  values dependent on temperature are used in the calculation, the initial chloride concentration necessary for passivity breakdown will vary more strongly with temperature, as observed experimentally.

We have approximated the potential term for migration with the concentration variation. Strictly speaking, this assumption is only valid for dilute

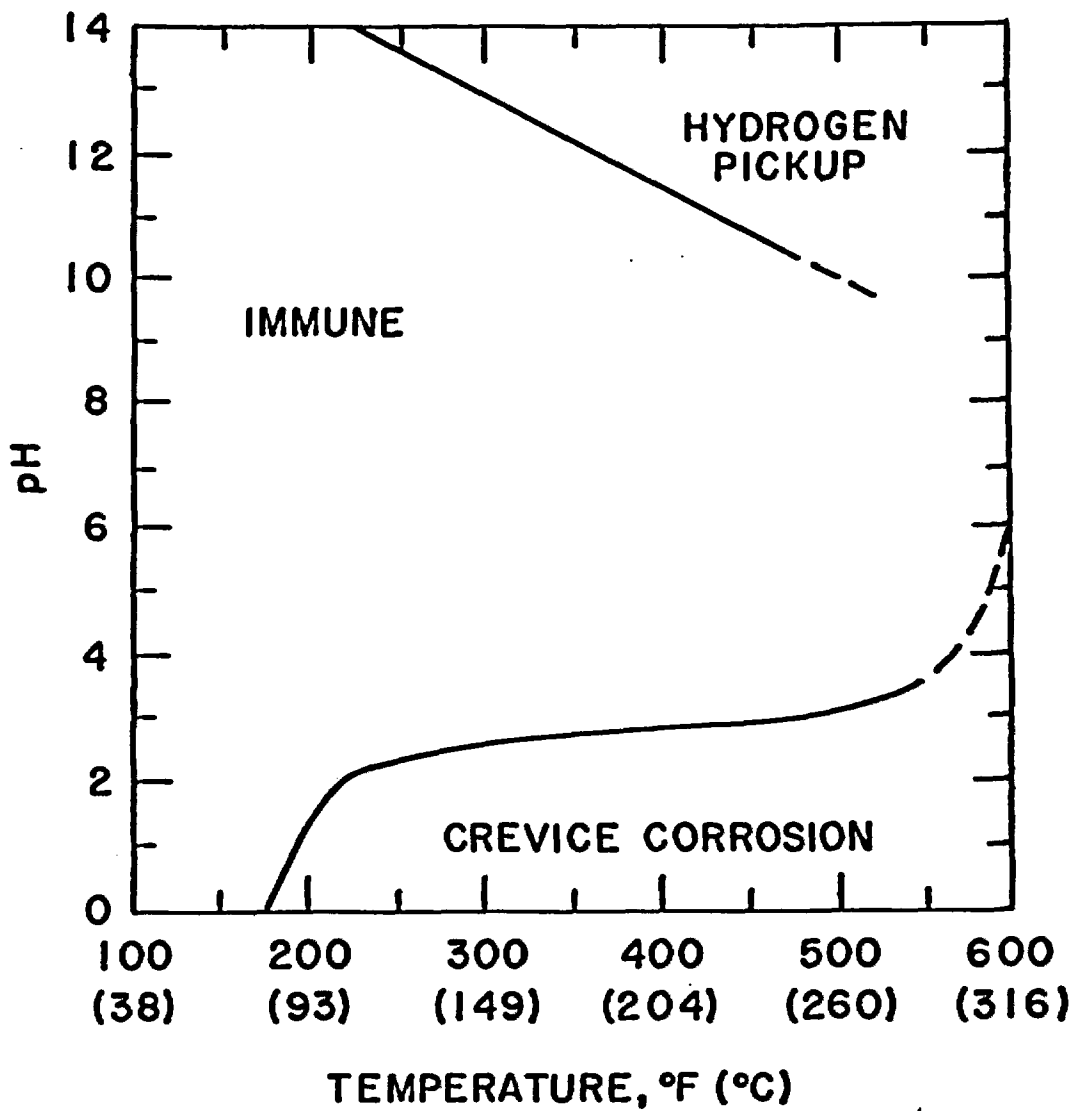


Figure 4. Immunity domains in temperature and pH necessary for passivity breakdown for CP titanium.<sup>18</sup>

solution. However, since we were concerned only with proton concentration, this assumption should be valid even though we have high anion concentrations.

Critical anion concentration for passivity breakdown has been assumed to be the near saturated concentration value. In diluted solutions, it may be possible that the critical anion concentration is smaller than the near saturated concentration. In this case, the initial anion concentration necessary for passivity will be reduced according to Equation (5).

## 5. CONCLUSIONS

A mass balance model was developed for the initiation of crevice corrosion. The basic process is the classical crevice corrosion mechanism obtained from immersion tests, surface analyses and electrochemical measurements. Initially the crevice potential rises because of the growth of a corrosion barrier oxide which consumes oxygen inside the crevice. After the maximum potential is reached, the barrier oxide stops growing and the following potential drop is governed by the solution chemistry change in the crevice. The potential drop resulting from oxygen depletion is the major source of potential change. A simple mass balance equation gives the potential rise as the oxide thickness is later increased. Simplified diffusion equations for oxygen, protons and anions were used to estimate the chemistry change inside the crevice. The potential drop was calculated using thermodynamic approximations. The calculated value was compared to an experimental value in order to estimate unknown parameters. The final equation was used to draw a map for crevice corrosion initiation in a temperature/anion concentration diagram. The calculated domains are consistent with experimental values. The equations also allow the chemistry inside the crevice to be estimated as a function of time.

6. REFERENCES

1. T. M. Ahn, R. Sabatini and P. Soo, "Immersion Tests and Surface Studies for the Crevice Corrosion of Grade-12 Titanium in a Brine Solution at 150°C." Preceding first paper.
2. H. Jain, T. M. Ahn and P. Soo, "An Electrochemical Study of Crevice Corrosion of Grade-12 Titanium in a Brine Solution." Preceding second paper.
3. J. L. Crolet and J. M. Defranoux, "Calculation of the Incubation Time of Crevice Corrosion in Stainless Steels; Corrosion Science 13, 575 (1973).
4. J. W. Oldfield and W. H. Sutton, "Crevice Corrosion of Stainless Steels," British Corrosion J. 13, 13 (1978).
5. ORNL-TM-4099, "Kinetics of Initiation of Crevice Corrosion of Titanium, Water Research Program Biannual Progress Report for the Period of March 15, 1966 to March 15, 1968," F. A. Posey and D. V. Subrahmanyam, Oak Ridge National Laboratory, 1973.
6. D. W. Sitarl and R. C. Alkire, "Initiation of Crevice Corrosion," J. Electrochemical Society 129, 482 (1982).
7. B. Vincentini, D. Sinigaglia and G. Taccani, "Crevice Corrosion: Calculation of the Voltage and Current Distribution Along the Crevice," Werkstoffe and Korrosion 22, 916 (1971).
8. T. R. Beck, "Initial Oxide Growth Rate on Newly Generated Surfaces," J. Electrochemical Society 129, 2501 (1982).
9. J. F. McAleer and L. M. Peter, "Instability of Anodic Oxide Films on Titanium," J. Electrochemical Society 129, 1252 (1982).
10. H. H. Uhlig, Corrosion and Corrosion Control, John Wiley and Sons, Inc., p. 11, p. 26, 1971.

11. J. O'M. Bockris and D. M. Drazic, Electrochemical Science, Barnes and Noble Books, New York, p. 141, 1972.
12. D. A. Vermilyea and C. S. Tedmon, Jr., "A Simple Crevice Corrosion Theory," J. Electrochemical Society 117, 437 (1970).
13. J. Newman, "Mass Transport and Potential Distribution in the Geometries of Localized Corrosion," in Localized Corrosion, Edited by R. W. Staehle, B. F. Brown, J. Kruger and A. Agrawal, NACE-3, 1974.
14. K. Shimogori, H. Sato and H. Tomari, "Crevice Corrosion of Titanium in NaCl Solutions in the Temperature Range 100 to 250 Degree C." J. of Japan Institute of Metals, 42(b), 1978.
15. Y. H. Li and S. Gregory, "Diffusion of Ions in Sea Water and in Deep-Sea Sediments," Geochimica et Cosmochimica Acta 38, 703 (1974).
16. A. Lerman, Geochemical Processes Water and Sediment Environments, John Wiley and Sons, Inc., p. 103, 1979.
17. Handbook of Chemistry and Physics, CRC Press, 62nd Edition, 1981-1982.
18. "Titanium Heat Exchangers for Service in Seawater, Brine, and Other Aqueous Environments," Titanium Information Bulletin from IMI, Birmingham, England, 1979.

ACKNOWLEDGEMENT

This work was performed under the auspices of the Nuclear Regulatory Commission (NRC). The author acknowledges program coordination by Dr. M. McNeil of the NRC. Also he acknowledges helpful discussions with Dr. P. Soo of Brookhaven National Laboratory.